Analytical Biochemistry xxx (2015) 1–7

Contents lists available at ScienceDirect

Analytical Biochemistry

journal homepage: www.elsevier.com/locate/yabio

Selective detection of silver ions using mushroom-like polyaniline and gold nanoparticle nanocomposite-based electrochemical DNA sensor

Yanqin Yang [a, b], Shuai Zhang [b], Mengmeng Kang [b], Linghao He [b], Jihong Zhao [a, b], Hongzhong Zhang [a, b], Zhihong Zhang [a, b, *]

[a] Henan Collaborative Innovation Center of Environmental Pollution Control and Ecological Restoration, Zhengzhou University of Light Industry, No. 166, Zhengzhou 450001, China
[b] Henan Provincial Key Laboratory of Surface and Interface Science, Zhengzhou University of Light Industry, No. 166, Zhengzhou 450001, China

ARTICLE INFO

Article history:
Received 19 June 2015
Received in revised form
5 August 2015
Accepted 6 August 2015
Available online xxx

Keywords:
AuNPs@PANI
Detection of silver ions
Electrochemical biosensor
Electrochemical impedance spectroscopy

ABSTRACT

A highly sensitive electrochemical DNA biosensor made of polyaniline (PANI) and gold nanoparticles (AuNPs) nanocomposite (AuNPs@PANI) has been used for the detection of trace concentration of Ag^+. In the presence of Ag^+, with the interaction of cytosine–Ag^+–cytosine (C–Ag^+–C), cytosine-rich DNA sequence immobilized onto the surface of AuNPs@PANI has a self-hybridization and then forms a duplex-like structure. The whole detection procedure of Ag^+ based on the developed biosensor was evaluated by electrochemical impedance spectroscopy. On semi-logarithmic plots of the log Ag^+ concentration versus peak current, the results show that the prepared biosensor can detect silver ions at a wide linear range of 0.01–100 nM ($R = 0.9828$) with a detection limit of 10 pM (signal/noise = 3). Moreover, the fabricated sensor exhibits good selectivity and repeatability. The detection of Ag^+ was determined by Ag^+ self-induced conformational change of DNA scaffold that involved only one oligonucleotide, showing its convenience and availability.

Ag^+ is a toxic heavy metal ion that is mainly used in electroplating, photographic, and imaging industries, graphic arts, dental and medical products, and electrical and electronic equipment [1,2]. It is also considered to be an important bioactive cation [3]. Within the scope of a low concentration, it exhibits low toxicity to living beings. However, Ag^+ ions are highly toxic to several aquatic organisms and humans in a high-concentration area [4]. It is reported that a concentration of silver in water sources higher than 1.6 nM is toxic for fish and microorganisms [5]. The Ag^+ ion standard of the U.S. Environmental Protection Agency and World Health Organization for drinking water is 0.5 μM [6]. Considering all of those potential problems, it is highly desirable to monitor its content level and develop a highly sensitive and selective detection of Ag^+ for environmental protection and human health.

Different approaches to detect and measure Ag^+ ions, such as flame atomic absorption [7], inductively coupled plasma–mass spectrometry [8], and inductively coupled plasma–atomic emission spectrometry [9] have been reported. However, these intensive instrumental methods require expensive and sophisticated instrumentation, which limits their practical applications. In addition, DNAzymes, as specific DNA molecules, possess the capacity of recognition toward organic molecules, proteins, cells, and heavy metal ions [10–12]. Although the negatively charged DNA can bind positively charged metal ions [13], some metal ions selectively anchor to some bases to form stable metal-mediated DNA duplexes such as thymine–Hg^{2+}–thymine [14,15], guanine–Cu^{2+}–guanine [16,17], and cytosine–Ag^+–cytosine (C–Ag^+–C)[1] [18,19] complexes. Substantial research has been devoted to the development of colorimetric biosensors, as well as fluorescent biosensors, using the specific interaction to detect Ag^+ [20,21]. Although these

* Corresponding author. Henan Provincial Key Laboratory of Surface and Interface Science, Zhengzhou University of Light Industry, No. 166, Zhengzhou 450001, China. Fax: +86 37186609676.
E-mail address: mainzhh@163.com (Z. Zhang).

[1] *Abbreviations used*: C–Ag^+–C, cytosine–Ag^+–cytosine complex; EIS, electrochemical impedance spectroscopy; NP, nanoparticle; PANI, polyaniline; AuNP, gold nanoparticle; AuNPs@PANI, PANI and AuNPs nanocomposite; GE, gold electrode; PBS, phosphate buffer solution; FT-IR, Fourier transform infrared; XRD, X-ray diffraction; XPS, X-ray photoelectron spectroscopy; FE-SEM, field emission scanning electron microscopy; CV, cyclic voltammetry; TEM, transmission electron microscopy; ssDNA, single-stranded DNA; LOD, limit of detection; RSD, relative standard deviation.

http://dx.doi.org/10.1016/j.ab.2015.08.010
0003-2697/

approaches have been successfully applied to the determination of Ag^+, drawbacks and limitations in practical applications still exist, including the complex synthesis of fluorophore materials, high background signal, poor selectivity toward other metal ions, and relatively low sensitivity. In contrast, electrochemical assays demonstrate their superiority in sensitivity, simple instrumentation, and easy miniaturization, which is very important in detection of Ag^+ ions [22,23]. Among the electrochemical approaches, electrochemical impedance spectroscopy (EIS) provides a powerful yet simple method of measuring changes in the bulk or interfacial properties of materials on an electrode surface, including surfaces that are sensitive to molecular recognition events. An ultra-low detection limit of 10 fM for Ag^+ was obtained using an EIS assay [24].

Recently, introducing inorganic nanoparticles (NPs) into conducting polymers has attracted research attention because of their simple and easy fabrication. Polyaniline (PANI), one of the most important conductive polymers, has been extensively investigated due to feasible synthesis [25,26], good environmental stability, and controllable electrochemical properties [27,28]. In terms of sensor applications, nanostructured PANI displays high sensitivity and rapid response time because of its highly effective surface area and short penetration depth for target analytes [29]. PANI-related nanocomposites were synthesized and fabricated as the biosensors to detect heavy metal ions, including Pb^{2+}, Cu^{2+}, Hg^{2+}, Cd^{2+} [30], and Pb^{2+} [31]. On the other hand, colloidal gold nanoparticles (AuNPs) are also excellent materials in sensor applications because these particles enhance electrode conductivity and facilitate electron transfer, thereby improving analytical selectivity and sensitivity [32,33]. Combining the advantages of PANI and AuNPs, including large surface area, high conductivity, and good biocompatibility [34], PANI and AuNPs nanocomposite (AuNPs@PANI) was synthesized and used as the sensitive layer for detection of hydrogen peroxide [35] and BCR/ABL fusion gene [36].

Here, AuNPs@PANI was synthesized and used to modify the surface of a gold electrode (GE) to construct an electrochemical single-stranded DNA biosensor, followed by sensitively detecting Ag^+ ions (Scheme 1). Because C–Ag^+–C interaction is key for the formation of the DNA scaffold as designed, the biocatalytic response with the relative amount of Ag^+ becomes the base of detecting Ag^+. In the current work, the bioelectrocatalytic signal of Q2 electrical contact of DNA and nanocomposite platform is effective for the signal amplification.

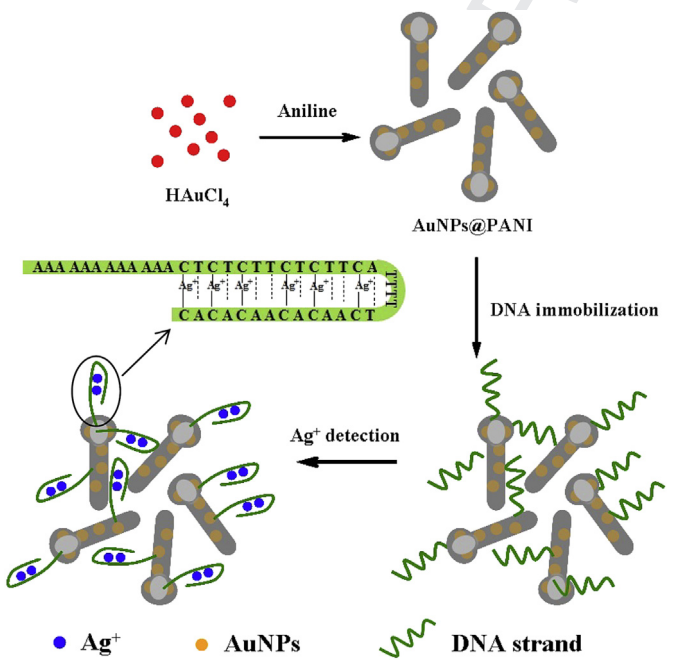

Scheme 1. Schematic diagram of the detection of Ag^+ ions using the developed electrochemical DNA biosensor based on AuNPs@PANI.

Materials and methods

Reagents and preparation of solutions

Aniline and $HAuC1_4$ were purchased from Aladdin Reagent (Shanghai, China). Ag^+ stock solution (1 mM) was prepared by dissolving $AgNO_3$ in 0.5% HNO_3. All other reagents were of analytical grade and used without further purification. All of the solutions were prepared using Milli-Q water (≥18.2 MΩ cm). DNA was obtained from SBS Genetech (Beijing, China).

The sequence of the oligonucleotides was as follows:

Probe DNA: 5′-AAA AAA AAA AAA CTC TCT TCT CTT CTT TTT TCA ACA CAA CAC AC-3′.

Stock DNA solutions were prepared in phosphate buffer solution (PBS), which was prepared by mixing 0.067 M Na_2HPO_4 and 0.067 M KH_2PO_4 in an 8:2 ratio of $v(Na_2HPO_4)/v(KH_2PO_4)$. The electrolyte solution was prepared immediately before use by dissolving 1.65 g of $K_3[Fe(CN)_6]$, 2.11 g of $K_4[Fe(CN)_6]$, 8 g of NaCl, and 0.2 g of KCl in 1 L of PBS.

Preparation of AuNPs@PANI

The preparation of AuNPs and PANI is described in the online Supplementary material. Synthesis of the AuNPs@PANI was completed through a one-step reduction process [37]. Briefly, 0.2 mL of 0.1 mol L^{-1} $HAuCl_4$ solution was added to 20 mL of water with 0.18 mL of aniline solution. The reaction was allowed to proceed for 16 h under stirring, and the final product was centrifuged at 10,000 rpm for 10 min. The precipitate was washed with water and then dried overnight at 60 °C. Finally, the AuNPs@PANI nanocomposite was obtained and stored at 4 °C before use.

Fabrication of biosensor based on AuNPs@PANI

Au electrodes (3 mm diameter) were polished with 0.05 μm alumina slurries, ultrasonically washed in ultrapure water, and electrochemically cleaned through a series of oxidation and reduction cycling in 0.5 M H_2SO_4 from −0.2 to 1.6 V (versus Ag/AgCl).

AuNPs@PANI (1.0 mg) was added to anhydrous ethanol and thoroughly sonicated until a homogeneous suspension of AuNPs@PANI was produced. Similarly, 1.0 mg L^{-1} AuNPs and 1.0 mg L^{-1} PANI homogeneous suspension was obtained. The suspension was stored under refrigeration at 4 °C. For contrast, the suspensions of 10 μL of 1.0 mg L^{-1} AuNPs, PANI, and AuNPs@PANI were dropped on the surface of the cleaned electrode to develop three electrochemical biosensors based on three nanomaterials, respectively. The modified electrodes were then dried at room temperature and immersed in 0.1 M PBS containing 100 nM DNA for 2 h. Finally, the probe DNA-modified electrodes were obtained.

Apparatus

Fourier transform infrared (FT-IR) spectra of the samples were acquired from samples in KBr pellets and using a Nicolet 5700 FT-IR instrument in the range of 400–4000 cm^{-1}. The X-ray diffraction

(XRD) spectra were obtained using a D8 Advance X-ray diffraction instrument (Germany) with a scanning 2θ angle of 10–80°. X-ray photoelectron spectroscopy (XPS) data were acquired using an AXIS HIS 165 spectrometer (Kratos Analytical, Manchester, UK) with a monochromatized Al KR X-ray source (1486.71 eV photons). Field emission scanning electron microscopy (FE-SEM) images were obtained using a JSM-6490LV scanning electron microscope (Japan). EIS and cyclic voltammetry (CV) were conducted using a CHI660D electrochemical workstation (Shanghai CH Instrument, China).

Electrochemical measurements

The electrochemical performance of the samples was measured by EIS and CV using 5 mM $K_3[Fe(CN)_6]/K_4[Fe(CN)_6]$ (1:1) electrolyte in a three-electrode cell. The measurement was conducted using a CHI660D electrochemical workstation at room temperature. An Ag/AgCl (saturated KCl) electrode, platinum slides, and an Au electrode were used as the reference, counter, and working electrodes, respectively. The impedance spectra were acquired at a frequency range from 0.01 Hz to 100 kHz and alternating current amplitude of 5 mV using $Fe(CN)_6^{3-}/Fe(CN)_6^{4-}$ as the redox couple. CV was carried out from −0.2 to 0.8 V at a scan rate of 100 mV s^{-1} at room temperature.

To form an electrical contacted DNA biosensor for Ag^+ detection, the composite Au electrode modified with AuNPs@PANI was immersed in 100 nM probe DNA for 2 h. After the self-hybridization of the DNA sequence in the presence of Ag^+, the electrical contacted DNA biosensor was obtained. For ultrasensitive detection of Ag^+, EIS of the biosensor were also carried out by incubating with different concentrations of Ag^+.

Results and discussion

Sensor design

Scheme 1 outlines the preparation processes of the DNA electrochemical biosensor based on AuNPs@PANI for detecting Ag^+ ions and the generation of the electrochemical signal. The single-strand oligonucleotide DNA acting as an anchor substrate on the composite AuNPs@PANI-GE platform is ready for detecting Ag^+. The DNA strand includes 8 complementary A–T base pairs and 12 mismatched C bases if folded. Once in the presence of Ag^+, 6 C–Ag^+–C base pairs will be formed and then cooperate to stabilize the duplex, in which case a duplex-like DNA scaffold is constructed. The concentration of Ag^+ ions added is directly relative to the extent of the EIS signal associated with the electrode, so a novel Ag^+ detection method is made by this efficient EIS process.

Chemical structure of AuNPs@PANI

Surface-sensitive XPS showed more information on the chemical composition of the AuNPs@PANI (Fig. 1). The peak at approximately 284.6 eV is assigned to the C–C/C–H bond, whereas the peak at 285.7 eV is possibly due to the C–N bond (Fig. 1A). The N 1s photoelectron spectrum shows peaks located at 398.3 and 400.0 eV that can be assigned to the N–C and N=C bonds, respectively (Fig. 1B). Two peaks at 83.95 and 87.65 eV correspond to the Au $4f_{7/2}$ and Au $4f_{5/2}$ energy levels, respectively [38,39] (Fig. 1C). No significant Au(III) component, with a binding energy at 87.0 eV, was observed. This result illustrates that the $HAuCl_4$ was reduced completely by aniline. The composites were mainly composed of C, N, and Au. These results demonstrate that the AuNPs@PANI was successfully synthesized.

Surface morphology of AuNPs@PANI

The morphology of the synthesized AuNPs@PANI material was investigated using FE-SEM and transmission electron microscopy (TEM) (Fig. 2). The SEM images of the AuNPs@PANI clearly show the microporous structure of the PANI [40]. TEM characterization was performed to study the presence of the AuNPs. The analysis was conducted by putting the samples on the Au grid. The TEM micrograph (Fig. 2D) clearly demonstrates the nanoparticles in the polymer matrices. A clear contrast between the AuNPs and the PANI was observed, indicating that the AuNPs were wrapped by the PANI. The AuNPs are spherical, with an average diameter of approximately 25 nm [41]. A lattice plane with a measured interplanar distance of 0.21 nm was observed (Fig. 2D).

The AuNPs that were incorporated into the PANI were confirmed from the powder XRD pattern of the composites, as shown in Fig. 2E. The presence of intense peaks correspond to the (111), (200), (220), (311), and (222) Bragg reflections of AuNPs [42]. The result shows that the AuNPs were present in the AuNPs@PANI.

Detection of Ag^+ ions using the electrochemical biosensors based on AuNPs, PANI, and AuNPs@PANI

The electrochemical performances of the nanomaterials were evaluated by EIS. The EIS spectra were analyzed using the software ZView2, and a nonlinear least square was used to fit and determine the parameters of the elements in an equivalent circuit (inset of Fig. S2 in Supplementary material). The equivalent circuit consists of solution resistance (R_s), charge transfer resistance (R_{ct}), constant phase element (CPE), and Warburg impedance (W_o). A typical impedance spectrum usually contains a linear part at low frequencies, which are related to diffusion, and a semicircle portion at high frequencies, which correspond to an electron transfer limited process. A large semicircle diameter represents a large interfacial charge transfer resistance R_{ct}.

Fig. 3A–C shows the EIS of the electrode at various stages for the detection of Ag^+ ions using the electrochemical biosensor of AuNPs, PANI, and AuNPs@PANI. A similar trend during the procedure of the Ag^+ detection was observed in three cases. After the nanomaterials were composited with the bare gold electrode, the R_{ct} value was increased, suggesting the generation of a surface with increased resistance of electron transfer at the interface between the composite electrode and electrolyte solution. In three cases, the coverage of single-stranded DNA (ssDNA) on the surface inhibited the access of the electrons to the modified surface, leading to low electron transfer efficiency of the system [43]. After ssDNA coordinated with Ag^+ ions, it increased the effect of the blocking layer Q3 on the electron transfer and resulted in the continuous decrease of the electrochemical activity and increase in R_{ct} [24].

To evaluate the efficiency of the detection of Ag^+ based on the different biosensors. The R_{ct} values for each stage in the detection of Ag^+ for three samples are shown in Fig. 3D. The differences in the R_{ct} values before and after the generation of a new layer adhesive (ΔR_{ct}) could represent its relative amount [44]. Among the three samples, the addition of PANI onto the GE led to the highest variation of R_{ct}, ΔR_{ct} = 0.84 kΩ. In cases of AuNPs- and PANI-based electrochemical biosensors, no substantial difference among ΔR_{ct} values of 0.52 and 0.59 kΩ for AuNPs and PANI biosensors, respectively, was observed after the DNA immobilization. As for AuNPs@PANI-based biosensor, the highest ΔR_{ct} value of 3.54 kΩ was obtained, indicating the lowest electron transfer at the interface between the modified electrode and the electrolyte solution. Subsequently, many more DNA molecules were anchored onto the surface of the AuNPs@PANI-based electrode. In aqueous solutions, the immobilization of the ssDNA onto AuNPs-modified electrode

Please cite this article in press as: Y. Yang, et al., Selective detection of silver ions using mushroom-like polyaniline and gold nanoparticle nanocomposite-based electrochemical DNA sensor, Analytical Biochemistry (2015), http://dx.doi.org/10.1016/j.ab.2015.08.010

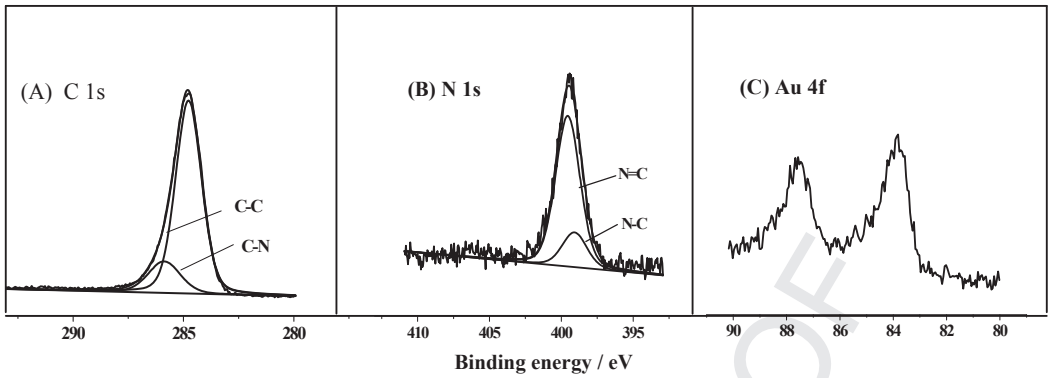

Fig.1. C 1s (A), N 1s (B), and Au 4f (C) core-level XPS spectra of AuNPs@PANI.

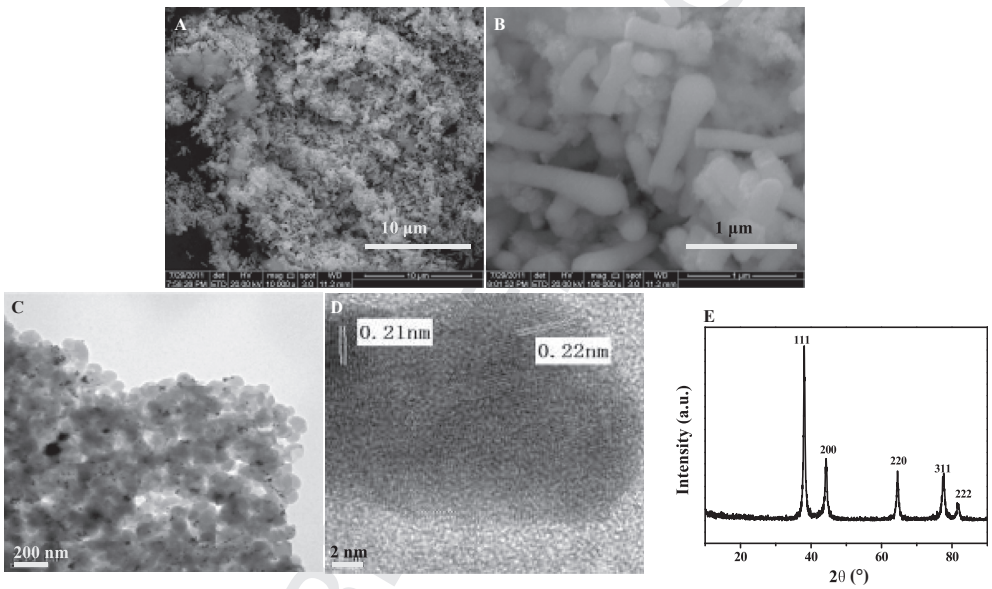

Fig.2. SEM images (A,B), TEM images (C,D), and XRD pattern (E) of AuNPs@PANI.

was mainly due to electrostatic adsorption [45,46]. Simultaneously, DNA molecules can be immobilized on the surface of PANI due to the electrostatic adsorption between the negative charges of phosphate groups in DNA strands and the positive charges of amino groups in PANI [47]. Consequently, the negative charged phosphate groups of the anchored DNA and the redox couple of $Fe(CN)_6^{3-/4-}$ lead to the slow electron transfer and further increases the R_{ct} value of the composite electrode [18]. Moreover, the difference of R_{ct} before and after the addition of Ag^+, ΔR_{ct}, is an important parameter to detect Ag^+ ions. Among three cases, the AuNPs@PANI shows good affinity for the ssDNA and further results in the highest variation of ΔR_{ct} (3.2 kΩ) in the presence of Ag^+. Other research demonstrates that Ag^+ can be adsorbed on AuNPs [46] and PANI [48] surface, leading to the directly sensitive detection of Ag^+. In the current work, EIS spectra of direct Ag^+ adsorption onto the AuNPs-, PANI-, and AuNPs@PANI-modified electrodes were carried out and are shown in Fig. S4 of the Supplementary material, suggesting the slight increase of the R_{ct} in the presence of Ag^+. On the other hand, the free C-rich part in the immobilized ssDNA would undergo a conformational change to form an intramolecular C—Ag^+—C duplex, resulting in the increase of the formed layer thickness. It may in turn reduce the electron transfer and increases the accompanying R_{ct} value [49]. Here, two effects take place at the same time and promote the increase of the R_{ct} value after the Ag^+ detection using the developed DNA sensor. Explicitly, the synergy effect between the AuNPs and PANI for bimolecular adsorption could be produced, leading to the detection of more Ag^+ ions.

To evaluate the efficiency of the electrostatic interaction between DNA strands and Ag^+, different DNA strands, including the DNA strands for the Cu^{2+} (DNA^{2+}_{Cu}) and Hg^{2+} (DNA^{2+}_{Hg}) detection, were immobilized onto the surface of the composite electrode modified with AuNPs@PANI, followed by the detection of Ag^+ (Fig. S5). The results show a slight change in R_{ct} values (0.13 kohm) of the composite electrode when DNA^{2+}_{Cu} was used. In case of DNA^{2+}_{Hg}, a ΔR_{ct} value of 0.96 kohm was observed and is approximately one-third that of the composite electrode with DNA^{+}_{Ag}. All of these demonstrate that the electrostatic interaction between Ag^+ and DNA strands was not substantial. The main interaction for the Ag^+ detection using the C-rich DNA sequence is mainly due to the specific C—Ag^+—C interaction.

Sensitivity of prepared electrochemical biosensor

After immobilizing the DNA on the developed sensor layer, the Ag^+ ions with different concentrations were subsequently incubated, as shown in Fig. 4A. The R_{ct} increased with increasing

Please cite this article in press as: Y. Yang, et al., Selective detection of silver ions using mushroom-like polyaniline and gold nanoparticle nanocomposite-based electrochemical DNA sensor, Analytical Biochemistry (2015), http://dx.doi.org/10.1016/j.ab.2015.08.010

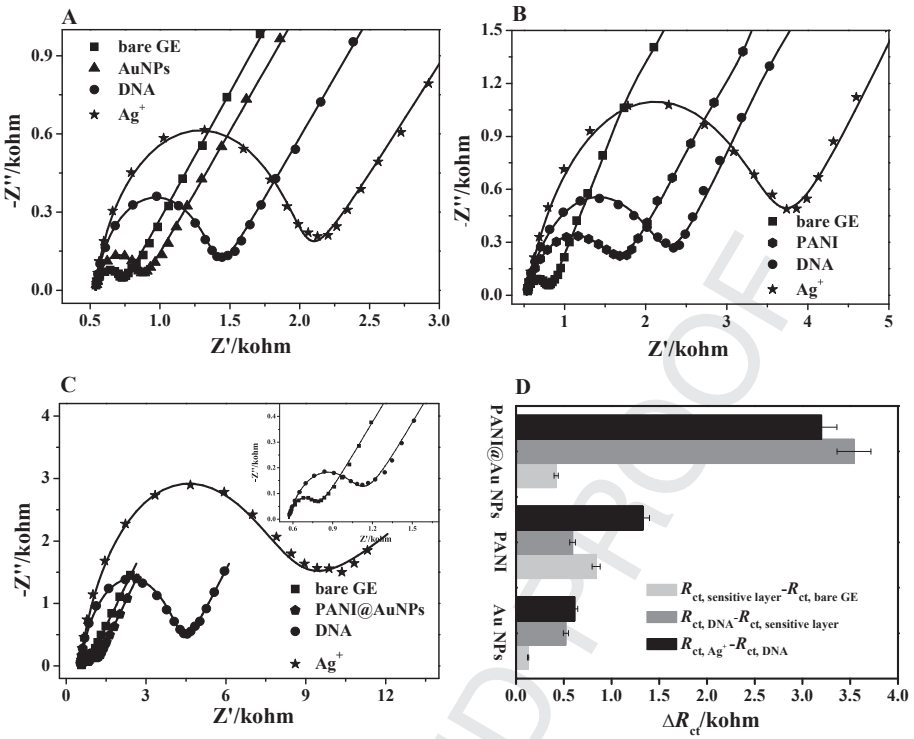

Fig.3. (A–C) Nyquist plots of EIS for bare GE (square curve) versus AuNPs (triangle curve) (A), PANI (hexagon curve) (B), and AuNPs@PANI modified GE (pentagon curve) (C), DNA immobilized onto the modified GE (circle curve), and the coordinated electrode after reacting with Ag^+ (star curve). The inset in panel C displays EIS spectra of GE and the composite electrode modified with AuNPs@PANI. (D) Variation in R_{ct} for each stage in the detection of Ag^+ was measured using the developed biosensors in which AuNPs, PANI, and AuNPs@PANI were used as the sensitive layers.

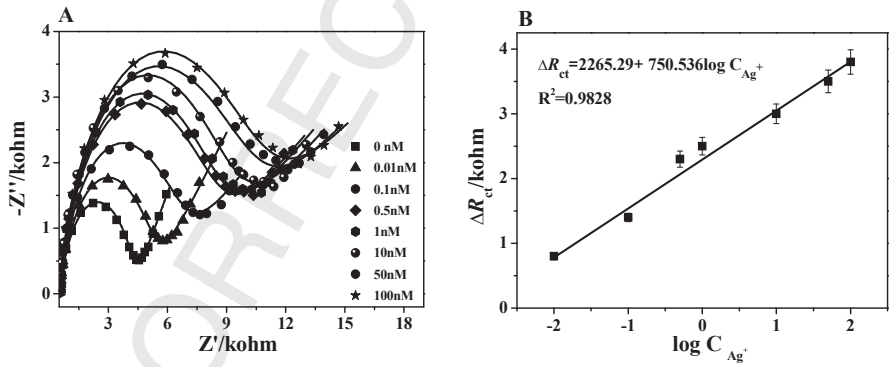

Fig.4. (A) Nyquist plots of EIS for detecting Ag^+. (B) Linear relationship between ΔR_{ct} and logarithm of Ag^+ concentration.

concentrations of the Ag^+ when the Ag^+ ions were detected. This behavior demonstrates the high sensitivity of the method.

The quantitative behavior of the assay was assessed by monitoring the dependence of the ΔR_{ct} on the amount of the Ag^+. The ΔR_{ct} caused by incubating each solution was proportional to the logarithmic concentration of the Ag^+ ions from 0.01 to 100 nM. Here, Freundlich adsorption equations are frequently employed to describe the adsorption process:

$$\Delta R_{ct} = a + b \log C_e, \quad (1)$$

where C_e is the concentration of Ag^+ (nM), ΔR_{ct} is the adsorption capacity (kohm), and a and b are the constants [50]. It shows that the ΔR_{ct} value was linear with the logarithm of Ag^+ concentration (Fig. 4B). The regression equation of the ΔR_{ct} was $\Delta R_{ct} = 2265.29 + 750.536 \log C_{Ag+}$ ($R^2 = 0.9828$). The sensitivity of the developed biosensor was determined based on the values obtained during detection and quantification limits. The limit of detection (LOD) is defined as the lowest concentration of an analyte that can be detected with acceptable accuracy. The LOD (signal/noise = 3) was calculated as 10 pM, which is not only superior to previously reported methods (see Table 1) [46,47,51,52] but also lower than the maximum level of Ag in drinking water permitted by the U.S. Environmental Protection Agency [6]. It was noted that the electrostatic interaction of Ag^+ with the negative charges of the DNA backbone was ignored in this case.

Selectivity and repeatability of developed biosensor

Selectivity was determined by substituting the Ag^+ in the incubation buffer with other single metal ions, including Hg^{2+}, Cu^{2+}, Ni^{2+}, Ba^{2+}, Pb^{2+}, Zn^{2+}, Mg^{2+}, Fe^{3+}, and Ag^+ (all at 1 μM). As shown

Table 1
Comparison of different Ag^+ detection methods.

Sensitive layer	Detection technique	Linear range (nM)	LOD (nM)	Reference
Polyaniline Langmuir–Blodgett film modified glassy carbon electrode	Linear scanning stripping voltammetry	0.6–1000	0.4	[46]
Exonuclease III activity on cytosine–cytosine (C–C) mismatches	Differential pulse voltammetry	0.1–120	0.03	[47]
Fe_3O_4@Au nanoparticles	Differential pulse voltammetry	117–17,700	59	[51]
Multi-walled carbon nanotubes derivate based on carbon paste electrode	Potentiometric	270–10^8	170	[52]
Polyaniline and gold nanoparticle nanocomposite	Electrochemical impedance spectroscopy	0.01–100	0.01	This work

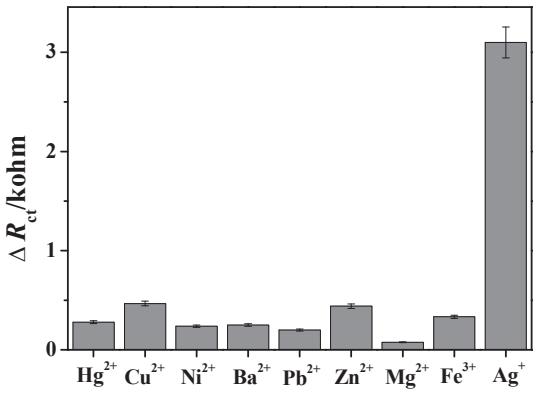

Fig.5. R_{ct} change in the presence of 1 μM of other metal ions and 100 nM Ag^+ ions.

in Fig. 5, the developed sensor showed remarkable response for the Ag^+ ions, and the sensor did not exhibit significant response to the other metal ions. This result demonstrates satisfactory selectivity in detecting the Ag^+ ions. The chemical stability of the DNA biosensor ensures that the sensor can be regenerated under proper conditions.

Because cysteine has a strong reaction with Ag^+ and can capture Ag^+ from C–Ag^+–C complexes, it was often used to regenerate the biosensor. In this work, the sensor was regenerated with 5 μM cysteine solution because of the disruption of the sandwich structure of C–Ag^+–C by cysteine, as shown in Fig. 6. The sensor was first challenged with 100 nM Ag^+ ions to obtain a response signal, followed by rinsing with cysteine solution. Afterward, the signal of the blank solution was recorded again. The biosensor showed good durability during tens of cycles, and the relative standard deviation (RSD) was 5.40%. This finding also indicates good repeatability.

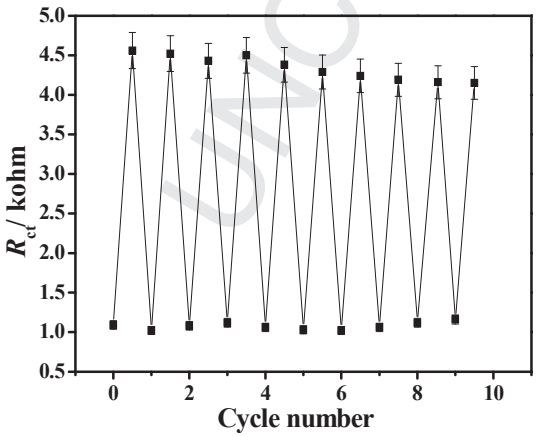

Fig.6. Reusability of EIS-based Ag^+ sensor challenged with 100 nM Ag^+ ions and washed with 5 mM cysteine.

Table 2
Analysis of Ag^+ in water samples detected by electrochemical biosensor based on nanocomposite of AuNPs@PANI.

Sample	Added (nmol)	Found (nmol)	Apparent recovery (%)	RSD (%)
River water	1	0.94	94.0	7.13
	5	5.06	101.2	6.74
	10	10.38	103.8	5.32
	50	49.36	98.7	4.95

Tests of real samples

The practical application of the developed biosensor for detecting Ag^+ ions was measured by determining the apparent recovery of the spiked Ag^+ ions in river water samples. The water sample was obtained from the Xushui River (Zhengzhou, China). The sample was then filtered through 0.2-μm membranes to remove impurities. Subsequently, standard Ag^+ solutions with different concentrations were added to the pretreated water sample. The spiked samples were analyzed separately using the designed sensor. The results are shown in Table 2. Apparent recovery values ranging from 94 to 103.8% were obtained, indicating that the designed sensor is applicable in analyzing Ag^+ in real water.

Conclusions

We have reported an ultrasensitive and selective electrochemical assay for the detection and quantitative analysis of silver ion based on AuNPs@PANI via the formation of C–Ag^+–C complex. ΔR_{ct}, before and after the addition of Ag^+, allowed the detection and quantitative analysis of Ag^+ with a low LOD of 10 pM within the range from 0.01 to 100 nM ($R = 0.9828$). Excellent selectivity toward interfering metal ions such as Hg^{2+}, Cu^{2+}, Ni^{2+}, Ba^{2+}, Pb^{2+}, Zn^{2+}, Mg^{2+}, Fe^{3+}, and Ag^+ can be achieved. The developed electrochemical biosensor could be regenerated by cysteine, which leads to the Ag^+ disassociated from the C–Ag^+–C complex. We expect that this strategy may offer a new approach for developing sensitive sensors for determination of various targets and could find wide applications in the environmental and biomedical fields.

Acknowledgments

This work was supported by the National Natural Science Foundation of China (NSFC, 51173172) and the Science and Technology Opening Cooperation Project of Henan Province (132106000076).

Appendix A. Supplementary material

Supplementary material for this article is available in the online version at http://dx.doi.org/10.1016/j.ab.2015.08.010.

References

[1] V.K. Bhardwaj, N. Singh, M.S. Hundal, G. Hundal, Mesitylene based azo-coupled chromogenic tripodal receptors: a visual detection of Ag(I) in aqueous medium, Tetrahedron 62 (2006) 7878–7886.

[2] H.J. Klasen, A historical review of the use of silver in the treatment of burns: II. Renewed interest for silver, Burns 26 (2000) 131–138.

[3] V. Sambhy, M.M. MacBride, R.B. Peterson, A. Sen, Silver bromide nanoparticle/polymer composites: dual action tunable antimicrobial materials, J. Am. Chem. Soc. 128 (2006) 9798–9808.

[4] M. Kumar, R. Kumar, V. Bhalla, Optical chemosensor for Ag^{+}, Fe^{3+}, and cysteine: information processing at molecular level, Org. Lett. 13 (2011) 366–369.

[5] S.Z. Mohammad, D. Afzali, M.A. Taher, Y.M. Baghelani, Ligandless dispersive liquid–liquid microextraction for the separation of trace amounts of silver ions in water samples and flame atomic absorption spectrometry determination, Talanta 80 (2009) 875–879.

[6] M. Hu, J. Fan, J. Cao, K. Song, H. Zhang, S. Sun, X. Peng, Enhanced fluorescent chemosensor for Ag^{+} in absolute aqueous solution and living cells: an experimental and theoretical study, Analyst 137 (2012) 2107–2111.

[7] M. Ghaedi, A. Shokrollahi, K. Niknam, E. Niknam, A. Najibi, M. Soylak, Cloud point extraction and flame atomic absorption spectrometric determination of cadmium(II), lead(II), palladium(II), and silver(I) in environmental samples, J. Hazard. Mater. 168 (2009) 1022–1027.

[8] F. Laborda, J.J. Lamana, E. Bolea, J.R. Castillo, Selective identification, characterization, and determination of dissolved silver(I) and silver nanoparticles based on single particle detection by inductively coupled plasma mass spectrometry, J. Anal. Atom. Spectrom. 26 (2011) 1362–1371.

[9] A. Väisänen, R. Suontamo, J. Silvonen, J. Rintala, Ultrasound-assisted extraction in the determination of arsenic, cadmium, copper, lead, and silver in contaminated soil samples by inductively coupled plasma atomic emission spectrometry, Anal. Bioanal. Chem. 373 (2002) 93–97.

[10] X.B. Zhang, R.M. Kong, Y. Lu, Metal ion sensors based on DNAzymes and related DNA molecules, Annu. Rev. Anal. Chem. 4 (2011) 105–128.

[11] X.H. Fang, W.H. Tan, Aptamers generated from cell–SELEX for molecular medicine: a chemical biology approach, Acc. Chem. Res. 43 (2010) 48–57.

[12] X. Fang, A. Sen, M. Vicens, W. Tan, Synthetic DNA aptamers to detect protein molecular variants in a high-throughput fluorescence quenching assay, ChemBioChem 4 (2003) 829–834.

[13] G.H. Clever, C. Kaul, T. Carell, DNA–metal base pairs, Angew. Chem. Int. Ed. 46 (2007) 6226–6236.

[14] J.R. Zhang, W.T. Huang, A.L. Zeng, H.Q. Luo, N.B. Li, Ethynyl and π-stacked thymine–Hg^{2+}–thymine base pairs enhanced fluorescence quenching via photoinduced electron transfer and simple and sensitive mercury ion sensing, Biosens. Bioelectron 64 (2015) 597–604.

[15] E. Xiong, L. Wu, J. Zhou, P. Yu, X. Zhang, J. Chen, A ratiometric electrochemical biosensor for sensitive detection of Hg^{2+} based on thymine–Hg^{2+}–thymine structure, Anal. Chim. Acta 853 (2015) 242–248.

[16] C. Ge, J. Chen, W. Wu, Z. Fang, L. Chen, Q. Liu, L. Wang, X. Xing, L. Zeng, An enzyme-free and label-free assay for copper(II) ion detection based on self-assembled DNA concatamers and SYBR Green I, Analyst 138 (2013) 4737–4740.

[17] C. Ocaña, N. Malashikhina, M. del Valle, V. Pavlov, Label-free selective impedimetric detection of Cu^{2+} ions using catalytic DNA, Analyst 138 (2013) 1995–1999.

[18] Z. Zhang, J. Yan, A signal-on electrochemical biosensor for sensitive detection of silver ion based on alkanethiol–carbon nanotube–oligonucleotide modified electrodes, Sens. Actuat. B 202 (2014) 1058–1064.

[19] G. Xu, G. Wang, Y. Zhu, L. Chen, X. He, L. Wang, X. Zhang, Amplified and selective detection of Ag^{+} ions based on electrically contacted enzymes on duplex-like DNA scaffolds, Biosens. Bioelectron. 59 (2014) 269–275.

[20] C.X. Tang, N.N. Bu, X.W. He, X.B. Yin, Functional nucleic acid-based electrochemiluminescent biosensor for interaction study and detection of Ag^{+} ions and cysteine, Chem. Commun. 47 (2011) 12304–12306.

[21] Y.H. Lin, W.L. Tseng, Highly sensitive and selective detection of silver ions and silver nanoparticles in aqueous solution using an oligonucleotide-based fluorogenic probe, Chem. Commun. (2009) 6619–6621.

[22] G. Yan, Y. Wang, X. He, K. Wang, J. Su, Z. Chen, Z. Qing, A highly sensitive electrochemical assay for silver ion detection based on unlabeled C-rich ssDNA probe and controlled assembly of MWCNTs, Talanta 94 (2012) 178–183.

[23] A.R. Zanganeh, M.K. Amini, A potentiometric and voltammetric sensor based on polypyrrole film with electrochemically induced recognition sites for detection of silver ion, Electrochim. Acta 52 (2007) 3822–3830.

[24] H. Gong, X. Li, Y-type, C-rich DNA probe for electrochemical detection of silver ion and cysteine, Analyst 136 (2011) 2242–2246.

[25] J. Huang, Syntheses and applications of conducting polymer polyaniline nanofibers, Pure Appl. Chem. 78 (2006) 15–27.

[26] C. Yang, J. Du, Q. Peng, R. Qiao, W. Chen, C. Xu, Z. Shuai, M. Gao, Polyaniline/Fe_3O_4 nanoparticle composite: synthesis and reaction mechanism, J. Phys. Chem. B 113 (2009) 5052–5058.

[27] M. Zhao, X. Wu, C. Cai, Polyaniline nanofibers: synthesis, characterization, and application to direct electron transfer of glucose oxidase, J. Phys. Chem. C 113 (2009) 4987–4996.

[28] R. Panigrahi, S.K. Srivastava, Ultrasound assisted synthesis of a polyaniline hollow microsphere/Ag core/shell structure for sensing and catalytic applications, RSC Adv. 3 (2013) 7808–7815.

[29] J. Huang, S. Virji, B.H. Weiller, R.B. Kaner, Polyaniline nanofibers: facile synthesis and chemical sensors, J. Am. Chem. Soc. 125 (2003) 314–315.

[30] X. Wang, Y. Shen, A. Xie, S. Chen, One-step synthesis of Ag@PANI nanocomposites and their application to detection of mercury, Mater. Chem. Phys. 140 (2013) 487–492.

[31] Z. Wang, E. Liu, D. Gu, Y. Wang, Glassy carbon electrode coated with polyaniline-functionalized carbon nanotubes for detection of trace lead in acetate solution, Thin Solid Films 519 (2011) 5280–5284.

[32] K. Saha, S.S. Agasti, C. Kim, X. Li, V.M. Rotello, Gold nanoparticles in chemical and biological sensing, Chem. Rev. 112 (2012) 2739–2779.

[33] J. Narang, N. Chauhan, C. Pundir, A non-enzymatic sensor for hydrogen peroxide based on polyaniline, multiwalled carbon nanotubes, and gold nanoparticles modified Au electrode, Analyst 136 (2011) 4460–4466.

[34] X. Feng, C. Mao, G. Yang, W. Hou, J.J. Zhu, Polyaniline/Au composite hollow spheres: synthesis, characterization, and application to the detection of dopamine, Langmuir 22 (2006) 4384–4389.

[35] S. Bao, M. Du, M. Zhang, H. Zhu, P. Wang, T. Yang, M. Zou, Facile fabrication of polyaniline nanotubes/gold hybrid nanostructures as substrate materials for biosensors, Chem. Eng. J. 258 (2014) 281–289.

[36] L. Wang, E. Hua, M. Liang, C. Ma, Z. Liu, S. Sheng, M. Liu, G. Xie, W. Feng, Graphene sheets, polyaniline, and AuNPs based DNA sensor for electrochemical determination of BCR/ABL fusion gene with functional hairpin probe, Biosens. Bioelectron. 51 (2014) 201–207.

[37] J. Han, L. Li, R. Guo, Novel approach to controllable synthesis of gold nanoparticles supported on polyaniline nanofibers, Macromolecules 43 (2010) 10636–10644.

[38] X. Wang, Y. Shen, A. Xie, S. Li, Y. Cai, Y. Wang, H. Shu, Assembly of dandelion-like Au/PANI nanocomposites and their application as SERS nanosensors, Biosens. Bioelectron. 26 (2011) 3063–3067.

[39] R.K. Pandey, V. Lakshminarayanan, A quick electrochemical approach for synthesizing the metal nanostructures stabilized with conducting polymers, Mater. Res. Bull. 50 (2014) 413–416.

[40] A. Stoyanova, S. Ivanov, V. Tsakova, A. Bund, Au nanoparticle–polyaniline nanocomposite layers obtained through layer-by-layer adsorption for the simultaneous determination of dopamine and uric acid, Electrochim. Acta 56 (2011) 3693–3699.

[41] M. Srivastava, S. Srivastava, N. Nirala, R. Prakash, A chitosan-based polyaniline–Au nanocomposite biosensor for determination of cholesterol, Anal. Methods 6 (2014) 817–824.

[42] Q. Yu, M. Shi, Y. Cheng, M. Wang, H.Z. Chen, Fe_3O_4@Au/polyaniline multifunctional nanocomposites: their preparation and optical, electrical, and magnetic properties, Nanotechnology 19 (2008) 265702.

[43] A. Noorbakhsh, A. Salimi, Development of DNA electrochemical biosensor based on immobilization of ssDNA on the surface of nickel oxide nanoparticles modified glassy carbon electrode, Biosens. Bioelectron. 30 (2011) 188–196.

[44] H. Torigoe, T. Kozasa, A. Ono, Detection of C:C mismatch base pair by fluorescence spectral change upon addition of silver(I) cation: toward the efficient analyses of single nucleotide polymorphism, Nucleic Acids Symp. Ser. (Oxf.) 50 (2006) 89–90.

[45] H. Gu, X.D. Su, K.P. Loh, Electrochemical impedance sensing of DNA hybridization on conducting polymer film-modified diamond, J. Phys. Chem. B 109 (2005) 13611–13618.

[46] Q. Liu, F. Wang, Y. Qiao, S. Zhang, B. Ye, Polyaniline Langmuir–Blodgett film modified glassy carbon electrode as a voltammetric sensor for determination of Ag^{+} ions, Electrochim. Acta 55 (2010) 1795–1800.

[47] G. Xu, G. Wang, X. He, Y. Zhu, L. Chen, X. Zhang, An ultrasensitive electrochemical method for detection of Ag^{+} based on cyclic amplification of exonuclease III activity on cytosine–Ag^{+}–cytosine, Analyst 138 (2013) 6900–6906.

[48] C.Y. Lin, C.J. Yu, Y.H. Lin, W.L. Tseng, Colorimetric sensing of silver(I) and mercury(II) ions based on an assembly of Tween 20-stabilized gold nanoparticles, Anal. Chem. 82 (2010) 6830–6837.

[49] G. Liu, Y. Yuan, S. Wei, D. Zhang, Impedimetric DNA-based biosensor for silver ions detection with hemin/G-quadruplex nanowire as enhancer, Electroanalysis 26 (2014) 2732–2738.

[50] J. Huang, K. Huang, S. Liu, Q. Luo, S. Shi, Synthesis, characterization, and adsorption behavior of aniline modified polystyrene resin for phenol in hexane and in aqueous solution, J. Colloid Interf. Sci. 317 (2008) 434–441.

[51] H. Yang, X. Liu, R. Fei, Y. Hu, Sensitive and selective detection of Ag^{+} in aqueous solutions using Fe_3O_4@Au nanoparticles as smart electrochemical nanosensors, Talanta 116 (2013) 548–553.

[52] T. Zhang, Y. Chai, R. Yuan, J. Guo, Nanostructured multi-walled carbon nanotubes derivate based on carbon paste electrode for potentiometric detection of Ag^{+} ions, Anal. Methods 4 (2012) 454–459.

Please cite this article in press as: Y. Yang, et al., Selective detection of silver ions using mushroom-like polyaniline and gold nanoparticle nanocomposite-based electrochemical DNA sensor, Analytical Biochemistry (2015), http://dx.doi.org/10.1016/j.ab.2015.08.010